Bioorganic Chemistry 90 (2019) 103087

Contents lists available at ScienceDirect

Bioorganic Chemistry

journal homepage: www.elsevier.com/locate/bioorg

Short communication

# Identification of chebulinic acid as a dual targeting inhibitor of protein tyrosine phosphatases relevant to insulin resistance

Sun-Young Yoon[a,1], Hyo Jin Kang[b,1], Dohee Ahn[a], Ji Young Hwang[a], Se Jeong Kwon[a], Sang J. Chung[a,*]

[a] School of Pharmacy, Sungkyunkwan University, Suwon 16419, Republic of Korea
[b] Department of Chemistry, Dongguk University, Seoul 100-715, Republic of Korea

ARTICLE INFO

*Keywords:*
Protein tyrosine phosphatases (PTPs)
Chebulinic acid
Type 2 diabetes
Glucose-uptake
PTPN9
PTPN11

ABSTRACT

Natural products as antidiabetic agents have been shown to stimulate insulin signaling via the inhibition of the protein tyrosine phosphatases relevant to insulin resistance. Previously, we have identified PTPN9 and DUSP9 as potential antidiabetic targets and a multi-targeting natural product thereof. In this study, knockdown of PTPN11 increased AMPK phosphorylation in differentiated C2C12 muscle cells by 3.8 fold, indicating that PTPN11 could be an antidiabetic target. Screening of a library of 658 natural products against PTPN9, DUSP9, or PTPN11 identified chebulinic acid (CA) as a strong allosteric inhibitor with a slow cooperative binding to PTPN9 ($IC_{50}$ = 34 nM) and PTPN11 ($IC_{50}$ = 37 nM), suggesting that it would be a potential antidiabetic candidate. Furthermore, CA stimulated glucose uptake and resulted in increased AMP-activated protein kinase (AMPK) phosphorylation. Taken together, we demonstrated that CA increased glucose uptake as a dual inhibitor of PTPN9 and PTPN11 through activation of the AMPK signaling pathway. These results strongly suggest that CA could be used as a potential therapeutic candidate for the treatment of type 2 diabetes.

## 1. Introduction

Diabetes is a significant health problem worldwide and type 2 diabetes accounts for over 90% of diabetic patients [1,2]. Type 2 diabetes is associated with insulin resistance in target organs as well as relative insulin deficiency caused by pancreatic β-cell dysfunction [1]. Since the long-term treatment of diabetic patients using hypoglycemic medications is often involved in renal failure and hepatotoxicity, it has become necessary to investigate new hypoglycemic agents from natural sources, which are considered to be less toxic and have fewer side effects than commonly used synthetic drugs [3,4]. Protein tyrosine phosphatases (PTPs) are a diverse family of enzymes that generally oppose activities of protein tyrosine kinases [5]. Controlling cellular protein tyrosine phosphorylation levels is associated with intracellular signaling pathways relevant to cell proliferation, differentiation, migration, and metabolism [6]. In particular, the PTPs such as PTPN1, PTPN9, PTPN11, PTPRF, PTPRS, and DUSP-9 are known to be involved in cellular insulin resistance associated with type 2 diabetes [6,7]. It has been shown that the loss of the protein tyrosine phosphatase, non-receptor type 1 (PTPN1, also named PTP1B) enhances insulin sensitivity and opposition to weight gain in mice, indicating that the inhibition of PTP1B is a potential therapeutic strategy for the treatment of type 2 diabetes and obesity [6,8]. In recent years, there has been an elevated interest in protein tyrosine phosphatase, non-receptor type 11 (PTPN11, also called SHP-2) related to adult acute myelogenous leukemia and human cancers including breast cancer, liver cancer, gastric cancer, oral cancer, and thyroid cancer [9]. Some reports have indicated that liver-specific PTPN11 knockout mice exhibit increased hepatic insulin activity and enhanced systemic insulin sensitivity via activation of the PI3K/Akt pathway [10,11]. PTPN11 has been known to bind C-terminal phosphotyrosine of insulin receptor substrate (IRS) which is an important regulatory event to attenuate insulin metabolic response [12]. Adenoviral-mediated depletion of protein tyrosine phosphatase, non-receptor type 9 (PTPN9, also named PTP-MEG2) in the liver of diabetic mice enhances insulin sensitization and reduces hyperglycemia [5,13].

Our previous studies revealed that PTPN9 and DUSP9 are potential antidiabetic targets and discovered their dual-targeting inhibitor, Ginkgolic acid [14]. In this study, PTPN11 knockdown enhanced AMPK phosphorylation, indicating that PTPN11 could be an antidiabetic target. Next, a library of 658 natural products was screened to identify multi-targeting inhibitors of PTPN9, DUSP9, or PTPN11 for antidiabetic

* Corresponding author.
*E-mail address:* sjchung@skku.edu (S.J. Chung).
[1] These authors contributed equally to this work.

https://doi.org/10.1016/j.bioorg.2019.103087
Received 28 February 2019; Received in revised form 17 June 2019; Accepted 25 June 2019
Available online 02 July 2019

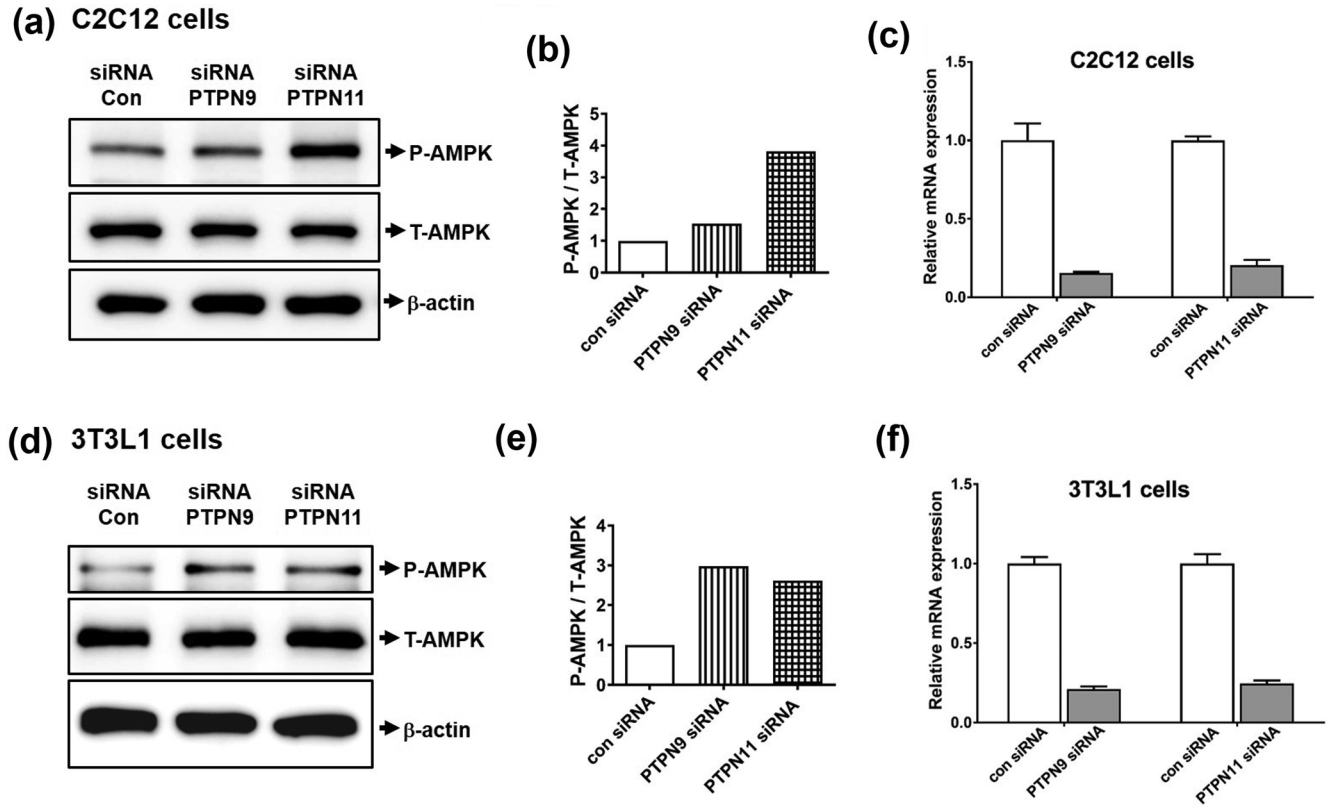


**Fig. 1.** Suppression of PTPN9 and PTPN11 increased AMPK phosphorylation. (a–f) C2C12 muscle cells (a–c) or 3T3-L1 preadipocytes (d-f) were transfected with PTPN9, PTPN11 siRNAs or scrambled siRNA as a control (con). After 24 h (d–f) or 48 h (a–c), cells were lysed and analyzed by Western blotting (a-b, d-e) or quantitative real-time PCR (c and f). (b and e) Quantification of phospho-AMPK and total-AMPK using ATTO image analysis software (CS analyzer 4). Results are expressed as the mean ± standard deviation.

**Table 1**
Kinetic constants for DiFMUP hydrolysis by PTPN9 and PTPN11.

| | [E] (nM) | $K_M$ (μM) | $V_{max}$ (μMmin$^{-1}$) | $k_{cat}$ (min$^{-1}$) | $k_{cat}/K_M$ (μM$^{-1}$ min$^{-1}$) |
|---|---|---|---|---|---|
| PTPN9 | 0.4 | 181.5 | 11.6 | $2.9 \times 10^4$ | 159.8 |
| PTPN11 | 5.0 | 91.4 | 4.8 | $9.6 \times 10^2$ | 10.5 |

natural products. Among the PTP-inhibitory compounds, chebulinic acid (CA) was identified as a potential antidiabetic drug that targeted PTPN9 and PTPN11 at the same time. CA isolated from the fruits of *Terminalia chebula* has been shown to prevent glutamate-induced HT22 mouse neuronal cell death via inhibition of oxidative stress and calcium influx [15]. However, its antidiabetic effects have not been investigated. Since insulin-stimulated glucose uptake by peripheral tissues such as skeletal muscle and adipocytes contribute to the maintenance of glucose homeostasis [16], we examined antidiabetic properties of CA in C2C12 muscle cells and 3T3-L1 adipocytes. Our cell-based studies demonstrated that CA could be a potential new therapeutic candidate for the treatment of type 2 diabetes.

## 2. Materials and methods

### 2.1. Cell culture

The methods used for culturing C2C12 muscle cells and 3T3-L1 preadipocytes obtained from American Type Culture Collection (ATCC, Manassas, VA, USA) have been described previously [17,18]. 3T3-L1 preadipocytes were cultured in high glucose Dulbecco's modified Eagle's medium (DMEM; Welgene, Gyeongsan-si, South Korea) containing 10% bovine calf serum (BCS; Thermo Fisher Scientific) and antibiotic-antimycotic solution (Welgene). C2C12 muscle cells were cultured in

**Table 2**
Inhibition of PTPN9 and PTPN11 by 20 μM ten natural compounds.

| PTPs | Inhibition (%) | | | | |
|---|---|---|---|---|---|
| | Amentoflavone | β-Carotene | Catechin gallate | Chebulinic acid | Emodin |
| PTPN9 | 42 | 20 | 50 | 89 | 41 |
| PTPN11 | 51 | 20 | 26 | 100 | 28 |
| PTPs | Inhibition (%) | | | | |
| | Galangin | Luteolin | Myricetin | Punicalin | Theaflavin |
| PTPN9 | 40 | 42 | 61 | 54 | 58 |
| PTPN11 | 21 | 28 | 25 | 43 | 25 |

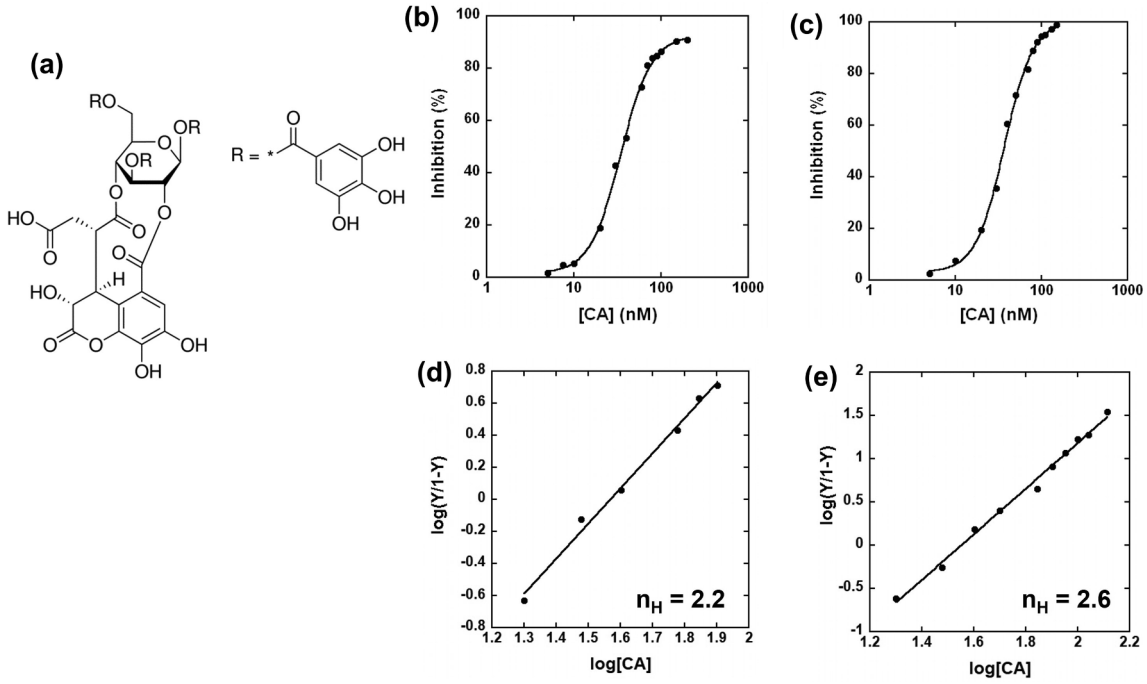


**Fig. 2.** PTPN9 and PTPN11 inhibition by CA treatment. (a) The chemical structure of CA. (b-c) The half-inhibitory concentrations ($IC_{50}$) were derived from the plots of inhibition (%) vs [CA] (nM) for PTPN9 (a, $IC_{50}$ = 34 nM) and PTPN11 (b, $IC_{50}$ = 37 nM), respectively. (d-e) The Hill coefficients ($n_H$), the slopes of the Hill plot using the Hill equation, were determined to be 2.2 for PTPN9 and 2.6 for PTPN11, respectively.

**Table 3**
Inhibition of PTPs by CA treatment.

| PTPs | PTPN1 | PTPN3 | PTPN9 | PTPN11 | PTPRA | PTPRE |
|---|---|---|---|---|---|---|
| Inhibition (%) | 13 | 40 | 89 | 100 | 40 | 48 |
| PTPs | PTPRF | PTPRK | PTPRS | DUSP1 | DUSP4 | DUSP9 |
| Inhibition (%) | 16 | 20 | 32 | 32 | 37 | 38 |

DMEM supplemented with 15% fetal bovine serum (FBS; Welgene) and antibiotic-antimycotic solution.

### 2.2. Cell differentiation

The methods used for differentiating 3T3-L1 preadipocytes and C2C12 cells have been described previously [17,18]. When 3T3-L1 preadipocytes reached 100% confluency, they were cultured in DMEM supplemented with 10% FBS, antibiotic-antimycotic solution, 0.5 mM isobutylmethylxanthine (IBMX; Merck KGaA, Darmstadt, Germany), 1 μM dexamethasone (Sigma-Aldrich, Saint Louis, Missouri, USA), and 5 μg/mL insulin (Merck KGaA, Darmstadt, Germany) for 2 days (days 0–2). Cells were then maintained in DMEM supplemented with 10% FBS, antibiotic–antimycotic solution, and 5 μg/mL insulin for a further 2 days (days 3–4) followed by culture in DMEM containing 10% FBS and antibiotic–antimycotic solution for an additional 4 days (days 5–8). When C2C12 muscle cells reached 100% confluency, cells were considered myoblasts in an early differentiation stage. They were cultured in DMEM supplemented with 2% horse serum (Thermo Fisher Scientific), antibiotic–antimycotic solution, and 5 μM insulin for 4 days. In all experiments, the culture medium was changed every other day.

### 2.3. Glucose uptake assay

The methods used for evaluating glucose-uptake in C2C12 muscle cells and 3T3-L1 preadipocytes have been described previously [17]. Differentiated cells were cultured in low-glucose DMEM (Gibco BRL) for 4 h and then incubated with CA or rosiglitazone in glucose-depleted DMEM (Gibco BRL) for 1 h. The cells were treated with the fluorescent glucose probe, 5 μM 2-[N-(7-nitrobenz-2-oxa-1,3-diazol-4-yl)amino]-2-deoxyglucose (2-NBDG; Thermo Fisher Scientific) for 30 min. After washing cells with FACS buffer (phosphate buffered saline (PBS, Welgene, Gyeongsan-si, South Korea), 1% FBS, 2 mM ethylenediaminetetraacetic acid (EDTA)), cell pellets were resuspended with FACS buffer and passed through a 40 μm cell strainer. For live/dead discrimination, propidium iodide (PI, Sigma-Aldrich) was used. PI-negative and 2-NBDG-positive cells were analyzed using a FACS Aria 2 instrument (BD, San Jose, CA, USA). To quantify 2-NBDG uptake, cells were washed with PBS and then the fluorescence intensity (excitation/emission = 485/535 nm) was measured on a fluorescence microplate reader (Victor™ X4, PerkinElmer, Waltham, MA, USA).

### 2.4. Overexpression and purification of recombinant PTPN9 and PTPN11

The methods used for overexpression and purification of PTPs have been described previously [19]. The N-terminal His6-tagged human PTPN9 and N-terminal MBP and C-terminal His6-tagged human PTPN11 genes were transformed into *E. coli* Rosetta (DE3) (Merck Millipore, Darmstadt, Germany). Expression of the recombinant PTPN9 or PTPN11 was induced by the addition of 0.1 mM or 1 mM IPTG; cells were grown at 18 °C for 16 h. Cells were then harvested by centrifugation (3570*g* at 4 °C for 15 min), washed with buffer A (50 mM Tris pH 7.5, 500 mM NaCl, 5% glycerol, 0.025% 2-mercaptoethanol, and 1 mM phenyl-methylsulfonyl fluoride (PMSF)), and then lysed by ultrasonication. After centrifugation (29,820*g* at 4 °C for 30 min), the supernatant was incubated with a cobalt affinity resin (TALON®, Takara Korea, Seoul, South Korea) on a rocker at 4 °C for 1 h. The resin was then washed with buffer A containing 10 mM imidazole. PTPN9 and PTPN11 were eluted with buffer A supplemented with 100 mM imidazole, and stored at −70 °C.

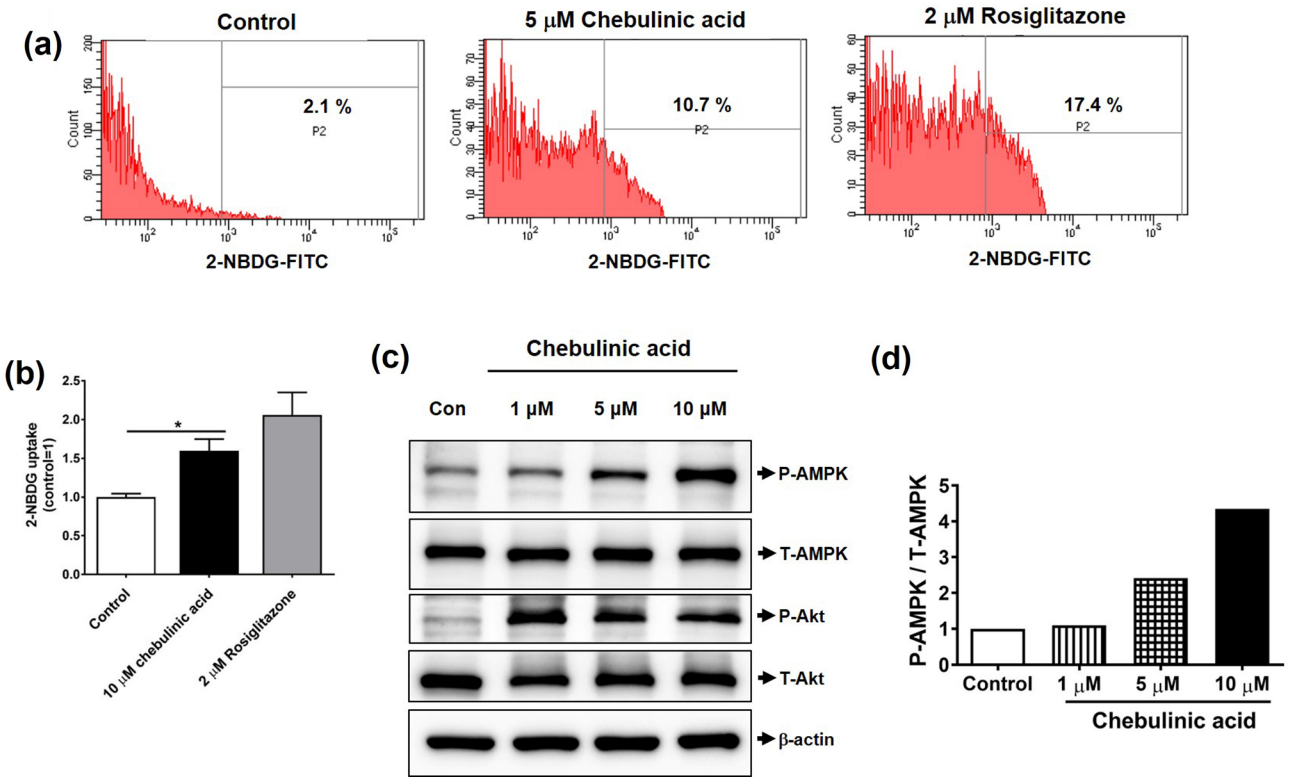


**Fig. 3.** CA treatment increased glucose uptake. (a) Differentiated 3T3-L1 preadipocytes were incubated for 1 h with 5 μM CA or rosiglitazone as a positive control. For live/dead discrimination, propidium iodide (PI) was used. PI-negative and 2-NBDG-positive cells were analyzed by FACS. (b) For the detection of 2-NBDG, cells were washed with PBS and then the fluorescence intensity (excitation/emission = 485/535 nm) was measured using a fluorescence microplate reader. Results are expressed as the mean ± the standard error of the mean. Data were analyzed using the two-tailed unpaired *t*-test. $^{*}P < 0.05$ compared to the control group. (c) During the differentiation of C2C12 muscle cells, the cells were incubated with 1, 5 or 10 μM CA. At day 6 after differentiation, cells were lysed, and Western blotting was performed using antibodies against phosphorylated AMPK, total AMPK, phosphorylated Akt, total Akt, or beta-actin. (d) Quantification of phospho-AMPK and total-AMPK using ATTO image analysis software (CS analyzer 4).

### *2.5. Measurement of enzymatic activities and half-inhibitory concentrations ($IC_{50}$) values*

The enzymatic activities of purified PTPN9 and PTPN11 were measured using 6,8-difluoro-4-methylumbelliferyl phosphate (DiFMUP) (100 μM), the most widely employed protein tyrosine phosphatase (PTP) substrate, as described previously [19]. To determine the $K_M$ values, PTPN9 (0.4 nM of the final concentration) and PTPN11 (5 nM of the final concentration) were added to reaction buffer (20 mM tris pH 7.0 (PTPN9) or 20 mM Bis-Tris pH 6.0 (PTPN11), 150 mM NaCl, 2.5 mM dithiothreitol (DTT), 0.01% Triton X-100) containing DiFMUP (800, 400, 200, 100, 50, 25, 12.5, or 6.25 μM) to a final volume of 100 μL in a 96 well-plate. Fluorescence intensities were measured continuously for 10 min (excitation/emission = 355/460 nm) using a Victor™ X4 multi label plate reader (Perkin Elmer), and $K_M$ values were determined by Lineweaver-Burk plots.

To estimate the inhibition of PTPN9 and PTPN11 by 658 natural compounds, PTPN9 (0.4 nM of the final concentration) and PTPN11 (5 nM of the final concentration) were added to solutions containing each of the compounds (20 μM) in reaction buffer with DiFMUP ($2 \times K_M$). To identify the mode of inhibition of CA, CA was added to DIFMUP (363 μM for PTPN9 or 182 μM for PTPN11) in reaction buffer. After addition of the enzymes PTPN9 (0.4 nM) and PTPN11 (5 nM), the progress curves were plotted for the product concentration over time. To estimate $IC_{50}$ values, various concentrations of CA and the both PTPs were pre-incubated for 30 min and then the solution containing DIFMUP (366 μM for PTPN9 or 144 μM for PTPN11) was added. $IC_{50}$ values were calculated using the sigmoid plots for the percentage of inhibition versus various concentrations of CA (KaleidaGraph, Synergy Software, PA, USA). The Hill coefficient ($n_H$) that measures the degree of cooperativity between CA and the both PTPs, was determined to be the slope of the Hill plot using the Hill equation [20].

### *2.6. Western blotting*

Proteins were extracted using a buffer containing 25 mM HEPES, 150 mM NaCl, 1% Triton X-100, 10% glycerol, 5 mM EDTA, 10 mM NaF, 2 mM $Na_3VO_4$, and protease inhibitor cocktail (Roche Korea, Seoul, South Korea). Proteins were separated by 10% sodium dodecyl sulfate-polyacrylamide gel electrophoresis and transferred to a polyvinylidene fluoride membrane (Merck KGaA, Darmstadt, Germany) using a wet transfer system. Membranes were incubated overnight at 4 °C with primary antibodies; anti-total AMPK, anti-phosphorylated AMPK, anti-total Akt, anti-phosphorylated Akt (Cell Signaling Technology, Beverly, MA, USA) and anti-beta-actin (AbFrontier, Seoul, South Korea). Membranes were then probed with anti-rabbit-IgG-horseradish peroxidase-conjugated secondary antibody (Santa Cruz Biotechnology, Dallas, TX, USA). Antibody–antigen complexes were detected using an ECL reagents (GE Healthcare Korea, Songdo, South Korea).

### *2.7. RNA interference*

Knockdown of PTPN9 and PTPN11 in 3T3-L1 preadipocytes and C2C12 muscle cells was performed using small interfering RNAs (siRNAs, Genolution Pharmaceuticals Inc., Seoul, South Korea). Scrambled siRNA was used as the negative control (Genolution Pharmaceuticals Inc., Seoul, South Korea). Transfections were

performed using Dharmafect (Dharmacon, GE Healthcare Korea, Songdo, South Korea) according to the manufacturer's instructions. The efficiency of PTPN9 and PTPN11 knockdown was measured by quantitative real time- polymerase chain reaction (qRT-PCR).

### 2.8. Quantitative real time-polymerase chain reaction (qRT-PCR)

Total RNA was isolated from 3T3-L1 preadipocytes and C2C12 muscle cells using the RNeasy Mini kit (Qiagen, Valencia, CA, USA) and treated with DNase (Qiagen) to remove genomic DNA. The total RNA (1 μg) was used to synthesize cDNA with the High Capacity Reverse Transcription kit (Applied Biosystems, Foster City, California, USA). PCR was performed on a CFX Connect Real-Time PCR Detection System (Bio-Rad, Hercules, CA, USA) using SsoAdvanced Universal SYBR green supermix (Bio-Rad) according to the manufacturer's instructions. Gene expression levels of PTPN9 and PTPN11 were normalized to levels of the control gene, GAPDH. Primer information is provided in Supplementary Table S1.

### 2.9. Statistical analysis

Statistical significance ($P < 0.05$) was determined by the two-tailed unpaired *t*-tests (GraphPad Software, San Diego, California).

## 3. Results and discussion

### 3.1. Suppression of PTPN9 and PTPN11 increased AMPK phosphorylation

In our previous findings, PTPN9 and DUSP9 were identified as potential antidiabetic targets using siRNAs [14]. To identify new antidiabetic targets, we analyzed the change in the phosphorylation level of AMPK upon the treatment with siRNAs. AMP-activated protein kinase (AMPK) has served as a marker for anti-diabetic effect as its activation leads to an improved insulin sensitivity [17,21]. Insulin binds to the insulin receptor on the surface of major insulin-sensitive tissues such as liver, adipose tissue and skeletal muscle to increase membrane translocation of GLUT4 [22], and particularly in skeletal muscle cells, a decrease of the glucose transporter 4, GLUT4, has been linked to cellular insulin resistance in animal models of diabetes [23,24]. We found that suppression of PTPN11 in C2C12 muscle cells and 3T3-L1 preadipocytes increased AMPK phosphorylation by Western blotting (Fig. 1a-b and d-e). Although PTPN9 knockdown in C2C12 muscle cells increased the phosphorylation of AMPK by only 53%, the down-regulation of PTPN11 increased the AMPK phosphorylation by 3.8-fold (Fig. 1a-b). The knockdown of PTPN9 by siRNA in 3 T3-L1 preadipocytes increased AMPK phosphorylation (Fig. 1d-e) similar to our previous report [14] but PTPN11 knockdown increased AMPK phosphorylation in relatively smaller extent than PTPN9 down regulation. These results indicate that contribution of the two PTPs to the AMPK phosphorylation is different in C2C12 and 3T3L1 cells. Efficient suppression of PTPN9 and PTPN11 was confirmed by quantitative RT-PCR (Fig. 1c and f). Different from PTPN9 and DUSP9 [14], however, concomitant knockdown of PTPN9 and PTPN11 did not show additive nor synergy effect to AMPK phosphorylation (data not shown). These results imply that PTPN11 could be a potential antidiabetic target to elevate glucose uptake in muscle tissue by inhibition thereof.

It has been reported previously that fumosorinone, a natural product isolated from insect fungi *Isaria fumosorosea,* increased glucose uptake and improved insulin resistance through inhibition of PTP1B, and that fumosorinone, a potent PTPN11 inhibitor, has been shown to inhibit tumor cell proliferation and reduce invasion of HeLa cells and MDA-MB-231 cells by downregulating Src signaling pathway [9,23,25]. However, it has not been tested if there is a correlation in the antidiabetic effect of fumosorinone and inhibitory activity of PTPN11. Current finding suggests that the antidiabetic effect of fumosorinone may be due to its dual inhibition of PTP1B and PTPN11.

### 3.2. PTPN9 and PTPN11 inhibition by CA

A library of 658 natural products was screened for inhibitors of PTPN9 and PTPN11 (Supplementary Table S2). For the high throughput screening of the natural product, the PTPs were overexpressed and purified by cobalt affinity resin (Supplementary Fig. S1). The catalytic activities of PTPs were measured using DiFMUP as a fluorogenic PTP substrate. The $K_m$ value of DiFMUP hydrolysis by PTPN11 was determined to be 91.4 μM (Table 1, Supplementary Fig. S2). At the initial screening, PTPs were added to 20 μM of each natural product with DIFMUP (363 μM for PTPN9 or 182 μM for PTPN11) and the fluorescence increase was monitored for 10 min. Based on the inhibition potency of the compounds, CA was selected for further study as a potential antidiabetic drug that targeted PTPN9 and PTPN11 at the same time (Table 2, Fig. 2a). CA showed a good inhibition of DiFMUP hydrolysis by both PTPN9 and PTPN11 rather than other PTPs tested here (Table 3). The progress curves of DiFMUP hydrolysis by PTPs were linear in the absence of inhibitor but hyperbolic progress curves were observed in the presence of CA, indicating that CA acted as a slow binding inhibitor against the both PTPs (Supplementary Fig. S3a-b). In addition, the plots of $1/k_{obs}$ (observed first-order rate constant) against 1/[CA] were hyperbolic, describing that slow-binding inhibition was due to slow isomerization of enzyme, followed by rapid binding of the inhibitor (Supplementary Fig. S3c-d) [26,27]. On the other hand, when the enzymes were pre-incubated with CA for 30 min and added to DiFMUP solution, the progress curves showed almost linear. Thus, measured initial velocities of the substrate hydrolysis by PTPN9 and PTPN11 were plotted against the concentrations of DiFMUP to determine kinetic constants of CA for the inhibition of PTPN9 and PTPN11. Based on these plots, the half-inhibitory concentrations ($IC_{50}$) of CA against PTPN9 and PTPN11 were estimated to be 34 and 37 nM, respectively (Fig. 2b-c). As the dose-response graph were sigmoidal rather than hyperbolic, CA was thought to bind PTPs in a cooperative manner and its inhibition constants ($K_i$ values) were not able to determine by conventional enzyme kinetics such as Lineweaver-Burk plot analysis. The data were replotted using Hill equation [20], resulting in Fig. 2d-e, where Y is a portion of complex formation between the corresponding enzyme and CA. The Hill coefficients ($n_H$) that describe the degree of cooperativity between ligand and protein were determined to be 2.2 for PTPN9 and 2.6 for PTPN11, respectively, indicating positive cooperation in CA binding to the both PTPs (Fig. 2d-e).

### 3.3. CA increased glucose uptake of differentiated 3T3-L1 adipocytes

We next examined the effect of CA on glucose uptake of differentiated 3T3-L1 adipocytes using the fluorescent glucose probe, 2-NBDG. Cells were treated with 10 μM CA or 2 μM rosiglitazone (an antidiabetic drug as a positive control [28]) for 1 h. After changing culture medium, the cells were treated with 2-NBDG for 30 min. After washing the cells, cell pellets were resuspended with FACS buffer and propidium iodide (PI) was used for live/dead discrimination. PI-negative and 2-NBDG-positive cells were analyzed using a FACS. We found that incubation with CA enhanced the percentage of 2-NBDG-positive cells among the living cells, as compared to control, suggesting that CA stimulated glucose uptake of the cells (Fig. 3a). These results were confirmed by the detection of cellular 2-NBDG using a fluorescence microplate reader. Cells were washed with PBS and then the fluorescence intensity (excitation/emission = 485/535 nm) was measured. CA treatment significantly increased fluorescence intensity compared with the control, revealing that incubation with CA enhanced glucose uptake of the cells (Fig. 3b). Rosiglitazone also increased the cellular fluorescence using a microplate reader or FACS, indicating that fluorescent probe was functional in our cell systems (Fig. 3a-b).

### 3.4. CA stimulates AMPK phosphorylation of differentiated C2C12 muscle cells

We investigated whether CA increases AMPK phosphorylation in differentiated C2C12 muscle cells. To this end, C2C12 muscle cells were differentiated in the presence of 1, 5, or 10 μM CA for 6 days and Western blotting was performed. CA treatment induced AMPK phosphorylation in a dose-dependent manner, as compared to control (Fig. 3c). In addition, incubation with CA enhanced Akt phosphorylation related to insulin stimulation (Fig. 3c-d) [29].

## 4. Conclusions

In this study, PTPN11 (SHP-2) was identified as a new antidiabetic target which is more significant in muscle cells rather than adipocytes. Here, for the first time, we demonstrate that CA can be a dual allosteric inhibitor with strong binding affinity to PTPN9 ($IC_{50}$ = 34 nM) and PTPN11 ($IC_{50}$ = 37 nM). The inhibitor showed a slow and positive cooperation when to bind the both enzymes. In addition, CA stimulated glucose uptake of the differentiated 3T3L1 adipocyte and C2C12 muscle cells through activation of the AMPK signaling pathway. Taken together, these results suggest that CA could be a potential therapeutic candidate for the treatment of type 2 diabetes.

## Declaration of Competing Interest

The authors declare no conflict of interest.

## Acknowledgements

This work was supported by the Ministry of Science and ICT through the National Research Foundation (NRF) of Korea (NRF-2012M3A9C4048775 and NRF-2017M3A9C8031995).

## Appendix A. Supplementary material

Supplementary data to this article can be found online at https://doi.org/10.1016/j.bioorg.2019.103087.

## References

[1] S. Chatterjee, K. Khunti, M.J. Davies, Type 2 diabetes, Lancet 389 (10085) (2017) 2239–2251.
[2] D. Huang, M. Refaat, K. Mohammedi, A. Jayyousi, J. Al Suwaidi, C. Abi Khalil, Macrovascular complications in patients with diabetes and prediabetes, Biomed. Res. Int. (2017, 2017,) 7839101.
[3] R.W. Snyder, J.S. Berns, Use of insulin and oral hypoglycemic medications in patients with diabetes mellitus and advanced kidney disease, Semin. Dial. 17 (5) (2004) 365–370.
[4] S.E. Kahn, S.M. Haffner, M.A. Heise, W.H. Herman, R.R. Holman, N.P. Jones, B.G. Kravitz, J.M. Lachin, M.C. O'Neill, B. Zinman, G. Viberti, Glycemic durability of rosiglitazone, metformin, or glyburide monotherapy, N. Engl. J. Med. 355 (23) (2006) 2427–2443.
[5] E.N. Gurzov, W.J. Stanley, T.C. Brodnicki, H.E. Thomas, Protein tyrosine phosphatases: molecular switches in metabolism and diabetes, Trends Endocrinol. Metab. 26 (1) (2015) 30–39.
[6] B.P. Kennedy, C. Ramachandran, Protein tyrosine phosphatase-1B in diabetes, Biochem. Pharmacol. 60 (7) (2000) 877–883.
[7] W.J. Hendriks, R. Pulido, Protein tyrosine phosphatase variants in human hereditary disorders and disease susceptibilities, Biochim. Biophys. Acta 1832 (10) (2013) 1673–1696.
[8] M. Elchebly, P. Payette, E. Michaliszyn, W. Cromlish, S. Collins, A.L. Loy, D. Normandin, A. Cheng, J. Himms-Hagen, C.C. Chan, C. Ramachandran, M.J. Gresser, M.L. Tremblay, B.P. Kennedy, Increased insulin sensitivity and obesity resistance in mice lacking the protein tyrosine phosphatase-1B gene, Science 283 (5407) (1999) 1544–1548.
[9] C. Chen, M. Cao, S. Zhu, C. Wang, F. Liang, L. Yan, D. Luo, Discovery of a novel inhibitor of the protein tyrosine phosphatase Shp2, Sci. Rep. 5 (2015) 17626.
[10] N. Nagata, K. Matsuo, A. Bettaieb, J. Bakke, I. Matsuo, J. Graham, Y. Xi, S. Liu, A. Tomilov, N. Tomilova, S. Gray, D.Y. Jung, J.J. Ramsey, J.K. Kim, G. Cortopassi, P.J. Havel, F.G. Haj, Hepatic Src homology phosphatase 2 regulates energy balance in mice, Endocrinology 153 (7) (2012) 3158–3169.
[11] K. Matsuo, M. Delibegovic, I. Matsuo, N. Nagata, S. Liu, A. Bettaieb, Y. Xi, K. Araki, W. Yang, B.B. Kahn, B.G. Neel, F.G. Haj, Altered glucose homeostasis in mice with liver-specific deletion of Src homology phosphatase 2, J. Biol. Chem. 285 (51) (2010) 39750–39758.
[12] M.G. Myers Jr., R. Mendez, P. Shi, J.H. Pierce, R. Rhoads, M.F. White, The COOH-terminal tyrosine phosphorylation sites on IRS-1 bind SHP-2 and negatively regulate insulin signaling, J. Biol. Chem. 273 (41) (1998) 26908–26914.
[13] C.Y. Cho, S.H. Koo, Y. Wang, S. Callaway, S. Hedrick, P.A. Mak, A.P. Orth, E.C. Peters, E. Saez, M. Montminy, P.G. Schultz, S.K. Chanda, Identification of the tyrosine phosphatase PTP-MEG2 as an antagonist of hepatic insulin signaling, Cell. Metab. 3 (5) (2006) 367–378.
[14] S.Y. Yoon, J.H. Lee, S.J. Kwon, H.J. Kang, S.J. Chung, Ginkgolic acid as a dual-targeting inhibitor for protein tyrosine phosphatases relevant to insulin resistance, Bioorg. Chem. 81 (2018) 264–269.
[15] J.H. Song, M.S. Shin, G.S. Hwang, S.T. Oh, J.J. Hwang, K.S. Kang, Chebulinic acid attenuates glutamate-induced HT22 cell death by inhibiting oxidative stress, calcium influx and MAPKs phosphorylation, Bioorg. Med. Chem. Lett. 28 (3) (2018) 249–253.
[16] R. Balasubramanian, B. Robaye, J.M. Boeynaems, K.A. Jacobson, Enhancement of glucose uptake in mouse skeletal muscle cells and adipocytes by P2Y6 receptor agonists, PLoS One 9 (12) (2014) e116203.
[17] M.S. Kim, H.J. Hur, D.Y. Kwon, J.T. Hwang, Tangeretin stimulates glucose uptake via regulation of AMPK signaling pathways in C2C12 myotubes and improves glucose tolerance in high-fat diet-induced obese mice, Mol. Cell. Endocrinol. 358 (1) (2012) 127–134.
[18] Y.L. Cho, J.K. Min, K.M. Roh, W.K. Kim, B.S. Han, K.H. Bae, S.C. Lee, S.J. Chung, H.J. Kang, Phosphoprotein phosphatase 1CB (PPP1CB), a novel adipogenic activator, promotes 3T3-L1 adipogenesis, Biochem. Biophys. Res. Commun. 467 (2) (2015) 211–217.
[19] S.Y. Lee, W. Kim, Y.G. Lee, H.J. Kang, S.H. Lee, S.Y. Park, J.K. Min, S.R. Lee, S.J. Chung, Identification of sennoside A as a novel inhibitor of the slingshot (SSH) family proteins related to cancer metastasis, Pharmacol. Res. 119 (2017) 422–430.
[20] M.I. Stefan, N. Le Novere, Cooperative binding, PLoS Comput. Biol. 9 (6) (2013) e1003106.
[21] G. Zhou, I.K. Sebhat, B.B. Zhang, AMPK activators–potential therapeutics for metabolic and other diseases, Acta. Physiol. (Oxf) 196 (1) (2009) 175–190.
[22] P.D. Brewer, E.N. Habtemichael, I. Romenskaia, C.C. Mastick, A.C. Coster, Insulin-regulated Glut4 translocation: membrane protein trafficking with six distinctive steps, J. Biol. Chem. 289 (25) (2014) 17280–17298.
[23] Z.Q. Liu, T. Liu, C. Chen, M.Y. Li, Z.Y. Wang, R.S. Chen, G.X. Wei, X.Y. Wang, D.Q. Luo, Fumosorinone, a novel PTP1B inhibitor, activates insulin signaling in insulin-resistance HepG2 cells and shows anti-diabetic effect in diabetic KKAy mice, Toxicol. Appl. Pharmacol. 285 (1) (2015) 61–70.
[24] V. Sarabia, L. Lam, E. Burdett, L.A. Leiter, A. Klip, Glucose transport in human skeletal muscle cells in culture. Stimulation by insulin and metformin, J. Clin. Invest. 90 (4) (1992) 1386–1395.
[25] L. Liu, J. Zhang, C. Chen, J. Teng, C. Wang, D. Luo, Structure and biosynthesis of fumosorinone, a new protein tyrosine phosphatase 1B inhibitor firstly isolated from the entomogenous fungus Isaria fumosorosea, Fungal. Genet. Biol. 81 (2015) 191–200.
[26] A.V. Bakker, S. Jung, R.W. Spencer, F.J. Vinick, W.S. Faraci, Slow tight-binding inhibition of prolyl endopeptidase by benzyloxycarbonyl-prolyl-prolinal, Biochem. J. 271 (2) (1990) 559–562.
[27] C.F. Chang, C.W. Ho, C.Y. Wu, T.A. Chao, C.H. Wong, C.H. Lin, Discovery of picomolar slow tight-binding inhibitors of alpha-fucosidase, Chem. Biol. 11 (9) (2004) 1301–1306.
[28] H.C. Gerstein, S. Yusuf, J. Bosch, J. Pogue, P. Sheridan, N. Dinccag, M. Hanefeld, B. Hoogwerf, M. Laakso, V. Mohan, J. Shaw, B. Zinman, R.R. Holman, Effect of rosiglitazone on the frequency of diabetes in patients with impaired glucose tolerance or impaired fasting glucose: a randomised controlled trial, Lancet 368 (9541) (2006) 1096–1105.
[29] N. Sharma, E.B. Arias, A.D. Bhat, D.A. Sequea, S. Ho, K.K. Croff, M.P. Sajan, R.V. Farese, G.D. Cartee, Mechanisms for increased insulin-stimulated Akt phosphorylation and glucose uptake in fast- and slow-twitch skeletal muscles of calorie-restricted rats, Am. J. Physiol. Endocrinol. Metab. 300 (6) (2011) E966–E978.